Süleyman Demirel Üniversitesi Fen Edebiyat Fakültesi Fen Dergisi https://dergipark.org.tr/sdufeffd
Süleyman Demirel University Faculty of Arts and Sciences Journal of Science e-ISSN: 1306-7575
Research Article, 2024, 19(1): 63-74, DOI: 10.29233/sdufeffd.1371161

# The Effect of Particle Size of Polyvinyl Alcohol/Bentonite Clay Mixture on the Radiation Shielding: A Monte Carlo Study

Tuğba Manici[1,2,*], Gökhan Algün[3], Namık Akçay[3], Bayram Demir[3]

[1]Radiotheraphy Program, Istanbul Sisli Vocational School, İstanbul, TURKEY
[2]Nuclear Physics, Institue of Graduate Studies in Science, Istanbul University, 34320, İstanbul, TURKEY
https://orcid.org/0000-0001-9616-6889
*corresponding author: tugba.manici@sisli.edu.tr
[3]Physics, Faculty of Science, Istanbul University, İstanbul, TURKEY
https://orcid.org/0000-0002-4607-3382
[3]Physics, Faculty of Science, Istanbul University, İstanbul, TURKEY
https://orcid.org/0000-0003-1660-213X
[3]Physics, Faculty of Science, Istanbul University, İstanbul, TURKEY
https://orcid.org/0000-0001-6815-6384

(Received: 06.10.2023, Accepted: 04.04.2024, Published: 27.05.2024)

***Abstract:*** Due to the harmful effects of ionizing radiation, shielding has become a crucial topic for radiation protection. Finding effective, non-toxic and low-cost shielding materials is imperative in ensuring the safety of individuals exposed to ionizing radiation. Whether a material is effective in shielding against radiation depends on the linear attenuation coefficient. In this study, linear attenuation coefficients were calculated using the MCNPX code for energy values of 81 keV (Ba-133), 140 keV (Tc-99m), 662 keV (Cs-137), 1173 keV, and 1332 keV (Co-60) by incorporating Bentonite Clay (BC) nanoparticles and micro-sized particles as additives into a Polyvinyl Alcohol (PVA) matrix. BC particles with a density of 50% were added to the PVA matrix using LAT and U cards. Simulations were performed with a mono-energetic source emitting $10^7$ particles and a narrow beam geometry, and the counts of particles with diameters of 50 nanometers and 50 micrometers were calculated using the F4 tally. When the results obtained from the simulation were compared, it was observed that as the diameters of the added particles decreased, their effectiveness in radiation shielding increased for each energy value. Among them, the 50 nm BC particles added at a rate of 50% in PVA showed the highest effect at 1332 keV, with a 9.5% increase compared to 50 μm BC particles.

***Key words:*** PVA, Bentonite Clay, Nanoparticles, Linear Attenuation Coefficient, MCNPX

## 1. Introduction

In recent years, the widespread use of radiation in various fields such as industry and medicine, coupled with the understanding of the potential biological effects resulting from exposure, underscores the importance of radiation protection. The realization that lead, commonly used in radiation shielding, can have toxic effects over time as a result of its interaction with radiation has led to a search for natural alternatives to lead. The pursuit of a new material that can provide effective radiation shielding while being easily obtainable, lighter, and more cost-effective than lead has kept research in this field current [1]. Additionally, studies have shown that nanoparticles are highly effective in radiation protection [2,3].

Due to the diversity of research topics, the use of mathematical approaches in radiation and materials science is increasingly on the rise. Among the various mathematical methods, Monte Carlo simulation stands out as one of the most preferred tools because

of its reliability and consistent approach, particularly when dealing with complex issues that may be difficult, expensive, or physically impossible to investigate experimentally. Dong et al. conducted research on the effects of nano-sized and micro-sized $WO_3$ particles added to E44 for gamma radiation shielding and found that nano-sized particles provided better radiation protection compared to micro-sized particles [4]. In another study, the mass attenuation coefficient of $WO_3$ added in nano and micro-sized particles within concrete was investigated using the MCNPX code, and it was observed that nano-sized particles provided the highest mass attenuation coefficient [5]. In a study conducted by Alavian at al., LDPE matrices were supplemented with W in four different sizes and at four different densities. Using the MCNP code, they investigated radiation shielding parameters and concluded that particle size had an inverse relationship with radiation shielding, and the ratio of the additive was a highly influential parameter [6]. In another study, $Bi_2O_3$ and $WO_3$ particles were examined within epoxy in nano and micro-sized using MCNP6, and similar results were obtained as in other studies [7].

Natural bentonite clays have also been investigated for their effectiveness in radiation shielding, in addition to heavy materials. Natural bentonite is derived from volcanic ash deposits formed as a result of volcanic eruptions and is naturally present at the nanometer scale. Furthermore, due to its high abundance and low cost, it is considered a good choice for this purpose [8,9,10]. In 2019, Hager et al. conducted experimental research on natural bentonite clays found in El Mutalla Mountain in Egypt, which naturally exist at the nanometer scale, under three different pressure values of 50, 100, and 150 bars, against 662 keV, 1173 keV, and 1332 keV gamma radiation. According to the Dynamic Light Scattering (DLS) measurement results of the obtained natural bentonite clay sample, the smallest size observed was 122 nm, representing 75% of the entire particle structure ranging from 122.4 to 220 nm. The study revealed that as the compression pressure of the bentonite clay increased, both density and linear attenuation coefficient also increased, with the highest linear and mass attenuation coefficients obtained under 150 bar pressure [8]. Elsafi at al. experimentally investigated the linear attenuation coefficients for four different bentonite clay samples at energies of 59 keV, 662 keV, 1173 keV, and 1332 keV gamma radiation. They concluded that natural bentonite clay provided the best shielding coefficient among the four different clays they studied, particularly at lower gamma energies [11].

Polyvinyl alcohol is an artificial polymer that has been used worldwide since the first half of the twentieth century, and it is produced from polyvinyl acetate through hydrolysis. It has been applied in various industries, including the industrial, medical, and food sectors, for the production of many end products such as resins, surgical threads, and food packaging materials that often come into contact with food [12,13]. The non-toxic and non-corrosive nature of PVA polymer, its water solubility, high optical transparency, and thermal stability make it a suitable matrix for optoelectronic and various other applications [14-16]. It has been demonstrated that a polymeric matrix containing suitable fillers exhibits favorable properties depending on the high surface area-to-volume ratio of the filler materials within the polymer matrix. An increase in the absorption/attenuation capabilities of a radiation shield is expected, while a decrease in the total weight is anticipated. Additionally, materials of this kind are expected to have higher compatibility and lower toxicity compared to lead [17,18].

In this study, the effects of changes in particle size on radiation shielding have been investigated. Polymeric matrix with a chemical formula of $C_2H_4O$ and a density of 1.19 $g/cm^3$, PVA [19] was used. Bentonite clays with particle sizes of 50 nm and 50 μm were added to the PVA matrix at a density ratio of 50% using LAT and U cards. Monte Carlo Simulation with the MCNP code was employed to simulate and examine the radiation

shielding parameters at energies of 81 keV (Ba-133), 140 keV (Tc-99m), 662 keV (Cs-137), 1173 keV, and 1332 keV (Co-60) which are the most commonly used gamma energies in medical applications. Due to the awareness of the harmful effects of ionizing radiation used in medical applications, protecting and finding a better useful shielding materials from such radiation is crucial to prevent exposure outside of the procedures.

## 2. Material and Method

### *2.1 Theoretical Approach*

The linear attenuation coefficient is calculated according to the Lambert-Beer law, which defines the attenuation of a mono-energetic beam as follows:

$$I = I_0 e^{-\mu x} \quad (1)$$

Here, $I$ represents the gamma radiation intensity after passing through the target material, $Io$ is the gamma radiation intensity from the source, $x$ is the thickness of the absorbing medium, and $\mu$ is the linear attenuation coefficient [20] Unit of the $\mu$ is $cm^{-1}$.

The effectiveness of gamma radiation shielding is described in terms of the Half-Value Layer (HVL) and Tenth-Value Layer (TVL) of the attenuating material. The unit for HVL and TVL is cm. HVL is defined as the thickness of the absorber material that reduces the intensity of gamma radiation to half of its value:

$$HVL = \frac{Ln2}{\mu} \quad (2)$$

TVL, which depends on the absorber material and photon energy of radiation, is defined as the thickness of the absorber material that reduces the intensity of gamma radiation to one-tenth of its initial value [21]:

$$TVL = \frac{Ln10}{\mu} \quad (3)$$

MFP, which is defined as the average distance between consecutive interactions, is mathematically the inverse of the linear attenuation coefficient. The relationship with photon energy explains why the number of interactions increases as the distance between interactions decreases. The MFP (in cm) for the shielding material is calculated using the following equation [22]:

$$MFP = 1/\mu. \quad (4)$$

### *2.2. Monte Carlo Code*

MCNPX (Monte Carlo N-Particle eXtended) is a code developed at the Los Alamos National Laboratory to simulate the behavior of particles such as neutrons, photons, electrons, and other particle types. The MCNPX code is based on the Monte Carlo method, which involves simulating the behavior of particles by tracking their interactions and movements through a defined geometry [23]. The code uses probability distributions and statistical methods to model physical processes that particles undergo, such as scattering, absorption, and nuclear reactions [5,24]. During this study, the simulation was run in photon mode only.

The simulation was carried out using LAT, U, SDEF, AXS, POS, PAR, ERG, and CELL cards. To determine the linear attenuation coefficient of the PVA/BC mixture against photons, mono-energetic beams were simulated. The selection of mono-energetic beams were from gamma-emitting radioactive sources, including 81 keV (Ba-133), 140 keV ($Tc\text{-}99^{m}$), 662 keV (Cs-137), 1173 keV, and 1332 keV (Co-60).

For the simulation with a narrow beam geometry, a spherical source with a 3 mm radius, lead collimators, and a target were set up as shown in Figure 1. The photon source is located within a cylindrical lead collimator with a radius of 3 mm and a length of 40 cm. The detector is positioned 43 cm away from the source on the same axis and has dimensions of 3x3x4 $cm^3$. The detector collimator is made of lead, with a diameter of 4.5 cm and a length of 10 cm. The modeled nano and micro-sized shielding materials were placed 40 cm away from the source, and they had dimensions of $4 \times 4 \times 0.2$ $cm^3$. Equation 5 was used for density calculations of the materials:

$$\frac{100}{\frac{m}{\rho_m} + \frac{f}{\rho_f}} \tag{5}$$

Here, m represents the percentage of the matrix, $\rho_m$ is the density of the matrix material, f represents the percentage of the filler material, and $\rho_f$ is the density of the filler material. The density of the new material consisting of a 50% PVA - 50% BC mixture is 1.6844 $g/cm^3$.

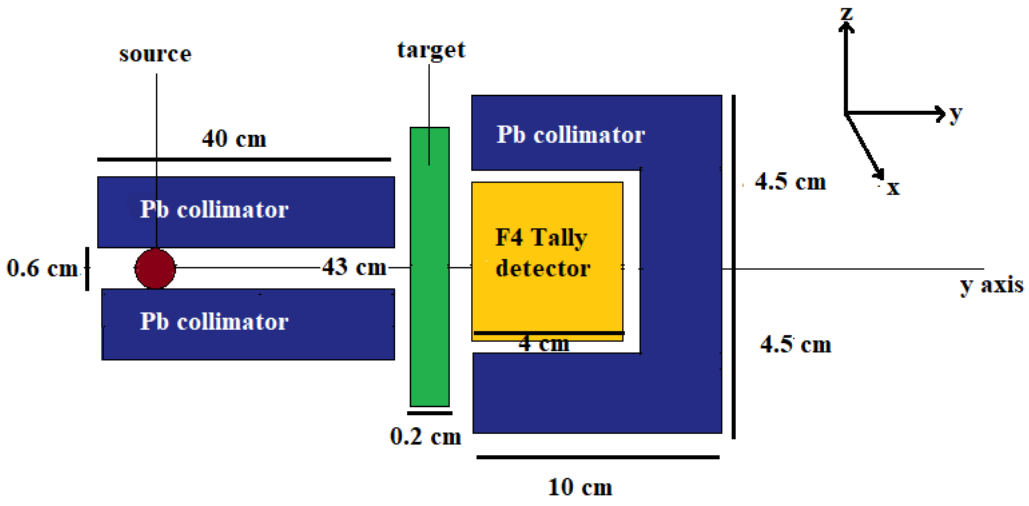


**Figure 1.** Schematic View of Simulation Geometry

### *2.2.1. Design of Nano and Micro Particles in the Matrix*

In this study, nano and micro particles were placed in the PVA matrix using lattice cards. The filler materials consisting of nano and micro-sized bentonite clays were defined within the PVA matrix as spheres located at the centers of cubes. Each micro and nano particle in the study was designed to have sizes of 50 micrometers and 50 nanometers, respectively. In Figure 2, an arrangement example for a 50% weight fraction is shown.

For the PVA matrix with 50% fraction of BC micro and nano particles, the size of each lattice cell was L, which is $1.4205 \times 10^{-02}$ cm and $1.4205 \times 10^{-05}$ cm, respectively. The F4 tally was used in the simulation to calculate the photon flux in the detector cell.

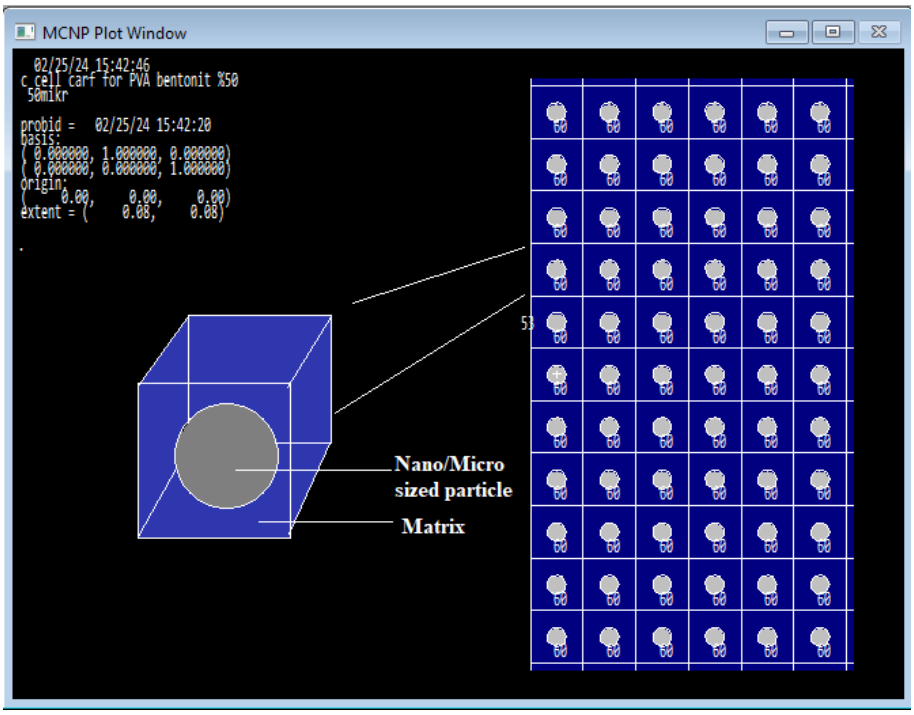


**Figure 2.** MCNP Screenshot of Nano/Micro BC Particles in PVA Matrix

As seen in Figure 3, the equidistant spacing between particles with a homogeneous distribution within the matrix is defined as "a." For the PVA matrix with a %50 density ratio of 50 nm diameter added particles, the distance "a" between two particles is $9.2054x10^{-06}$ cm. For particles with a diameter of 50 µm added to the matrix, the distance "a" between two particles is $9.2054x10^{-03}$ cm.

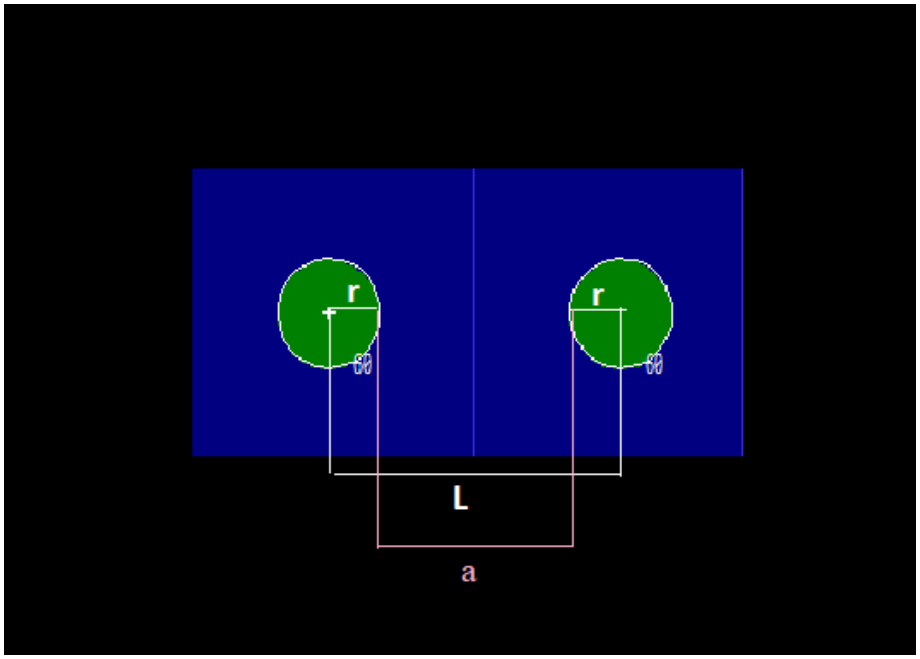


**Figure 3.** Inter-particle Distance Representation

The F4 tally evaluates the number of photons entering a cell in MeV/cm$^2$. The relative statistical errors of the MC results are less than %1 [25]. Table 1 contains the elemental weight fractions of bentonite clay and PVA used in the simulation. These data were used for material definitions in the simulation [19,26].

**Table 1.** Elemental Mass Fractions Used in MCNPX

| | **Bentonite Clay** | **PVA** |
|---|---|---|
| **Density** | 2.881 g/cm$^3$ | 1.19 g/cm$^3$ |
| H | 0.007977 | 0.091520 |
| C | - | 0.545296 |
| O | 0.525272 | 0.363184 |
| Na | 0.012504 | - |
| Mg | 0.018654 | - |
| Al | 0.088209 | - |
| Si | 0.308240 | - |
| P | 0.000130 | - |
| K | 0.004445 | - |
| Ca | 0.010133 | - |
| Ti | 0.000832 | - |
| Mn | 0.000998 | - |
| Fe | 0.022607 | - |

## 3. Results

### *3.1. MCNPX and XCOM Validation*

In order to test the reliability of the results obtained with the geometry designed using the Monte Carlo code, the linear attenuation coefficients of pure PVA ($C_2H_4O$) polymer were calculated using the MCNPX code at different energy values. The linear attenuation coefficients obtained at 81 keV, 140 keV, 662 keV, 1173 keV, and 1332 keV energies were compared with the National Institute of Standards and Technology (NIST) data [27]. As shown in Table 2 , there is a close agreement between the Monte Carlo results and the NIST data. The maximum approximate difference between Monte Carlo and NIST values is about %0.49. Therefore, the created Monte Carlo model has been validated for further simulations in the study.

**Table 2.** MCNPX AND XCOM Values of Linear Attenuation Coefficients of PVA (d=1.19 g/cm$^3$) and % Difference Between the Results

| **Energy (keV)** | **μ-XCOM( 1/cm)** | **μ-MCNPX ( 1/cm)** | **% DIFFERENCE** |
|---|---|---|---|
| 81 | 0.2099 | 0.2094 | 0.2382 |
| 140 | 0.1787 | 0.1783 | 0.2238 |
| 662 | 0.1001 | 0.0996 | 0.4995 |
| 1173 | 0.0762 | 0.0761 | 0.1312 |
| 1332 | 0.0714 | 0.0712 | 0.2801 |

### *3.2. Comparison between MCNPX and Other Studies*

The study conducted by Elsafi and colleagues involved four types of clay: Red, ball, kaolin, and bentonite, obtained from stone quarries in the Aswan, Abuznima, and Fayoum governorates of Egypt. These samples were sieved to a size of 100 μm, mixed thoroughly with water, divided into slices, and then dried in the sun to obtain them. Subsequently, they obtained linear attenuation coefficients for 662 keV, 1173 keV, and 1332 keV gamma sources. Table 3 shows the linear attenuation coefficients for these four different types of clay and, additionally, the linear attenuation coefficients for ordinary concrete as found in the study by Cape Town for bentonite clay and in Bashter's study [28] for ordinary concrete. Figure 4 presents a comparison of the data from Table 3.

**Table 3.** Comparison of Linear Attenuation Coefficients of Pure Bentonite Clay with Previously Published Data

| ENERGY (KEV) | LAC (1/cm) | | | | | |
|---|---|---|---|---|---|---|
| | RED CLAY | BALL CLAY | KAOLIN CLAY | BENTONITE CLAY | ORDINARY CONCRETE | THIS STUDY (BC) |
| | [11] | [11] | [11] | [11] | [28] | MCNPX |
| **81** | - | - | - | - | - | 0.5762 |
| **140** | - | - | - | - | - | 0.4199 |
| **662** | 0.1608 | 0.1524 | 0.1525 | 0.1608 | 0,1513 | 0.2222 |
| **1173** | 0.1224 | 0.1161 | 0.1161 | 0.1221 | 0.1366 | 0.1695 |
| **1332** | 0.1101 | 0.1087 | 0.1088 | 0.1146 | 0.1279 | 0.1587 |

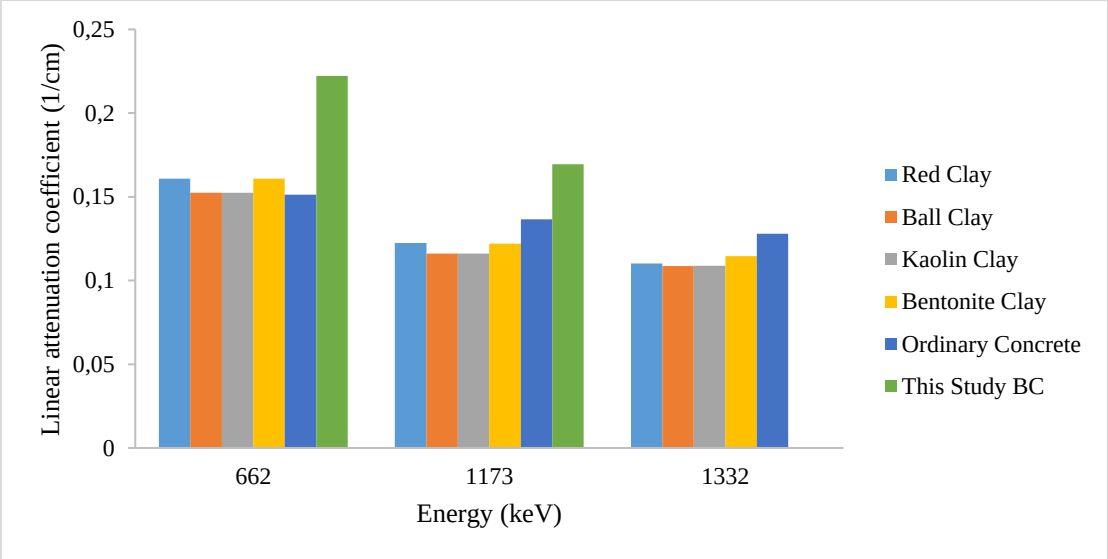


**Figure 4.** Comparison of Linear Attenuation Coefficients of Pure Bentonite Clay with Previously Published Data

### *3.3. The Effect of Particle Size on Linear Attenuation Coefficients*

Table 4 presents the calculated linear attenuation coefficients for samples of bentonite clay added to PVA with a 50% weight ratio at 81, 140, 662, 1173, and 1332 keV gamma energies, along with the percentage difference between nano and micro-sized particles. When looking at Figure 5, which contains separate comparisons for each energy value, it can be observed that for the same proportion of added BC, the linear attenuation coefficient increases as the particle size decreases. The increased linear attenuation coefficients due to a decrease in particle size exhibit the same increasing trend for each energy. The highest linear attenuation coefficient was obtained for nano-sized BC added at 81 keV energy, with a value of 0.230 $cm^{-1}$. When considering the exchange between nano and micro particles at the same energy values, the highest difference occurs at 1332 keV with a percentage difference of %8.974. In Table 5, the linear attenuation coefficients and percentage differences are presented for pure PVA and PVA with nano-sized BC added at the same energies. Here, the addition of nano-sized BC results in an increase in the linear attenuation coefficient for each energy value, with the highest difference observed at 662 keV with a percentage difference of %15.384.

Figure 6 compares the linear attenuation coefficients of pure PVA, PVA with 50 nm-BC added at a 50% ratio, and PVA with 50 μm-BC added at a 50% ratio. It can be observed that nano-sized BC added provides the highest effect among these materials in terms of linear attenuation coefficients.

**Table 4.** Comparison of Linear Attenuation Coefficients and Percentage Difference Values of BC's Micro and Nano Samples at Different Photon Energies (keV)

| ENERGY (keV) | μ-LAC (%50 PVA+50 μm BC) | μ-LAC (%50 PVA+50 nm BC) | % DIFFERENCE |
|---|---|---|---|
| 81 | 0.221 | 0.230 | 3.913 |
| 140 | 0.180 | 0.191 | 5.759 |
| 662 | 0.114 | 0.117 | 2.564 |
| 1173 | 0.075 | 0.078 | 3.846 |
| 1332 | 0.071 | 0.078 | 8.974 |

**Table 5.** Comparison of Linear Attenuation Coefficients and Percentage Difference Values of BC's Nano Samples and Pure PVA at Different Photon Energies (keV).

| ENERGY (keV) | μ-LAC (PURE PVA) | μ-LAC (%50 PVA+50 nm BC) | % DIFFERENCE |
|---|---|---|---|
| 81 | 0.209 | 0.230 | 9.130 |
| 140 | 0.178 | 0.191 | 6.806 |
| 662 | 0.099 | 0.117 | 15.384 |
| 1173 | 0.075 | 0.078 | 3.846 |
| 1332 | 0.071 | 0.078 | 8.974 |

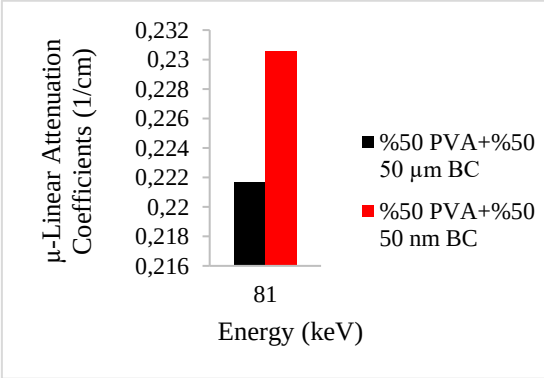


**(a)**

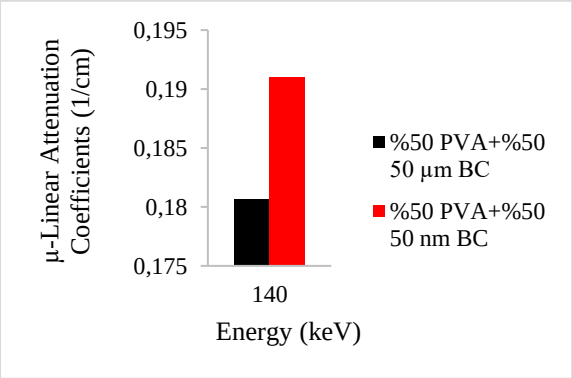


**(b)**

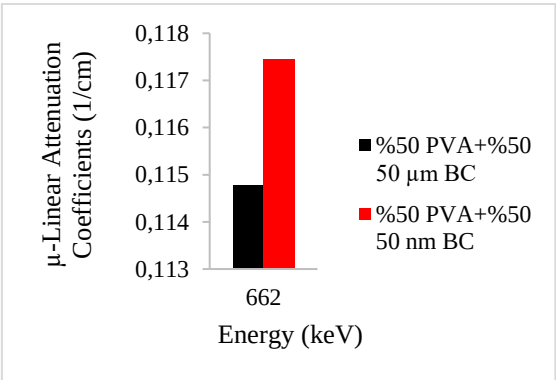


**(c)**

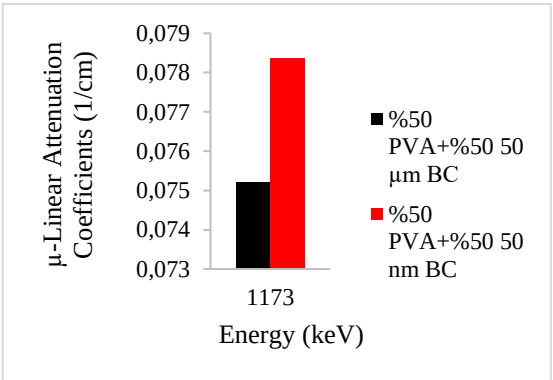


**(d)**

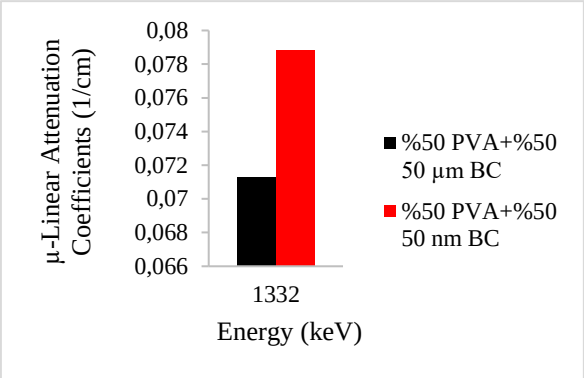


**(e)**

**Figure 5.** Comparison of Linear Attenuation Coefficient of Micro and Nano Samples for Photon Shielding at Different Energy Levels (keV)

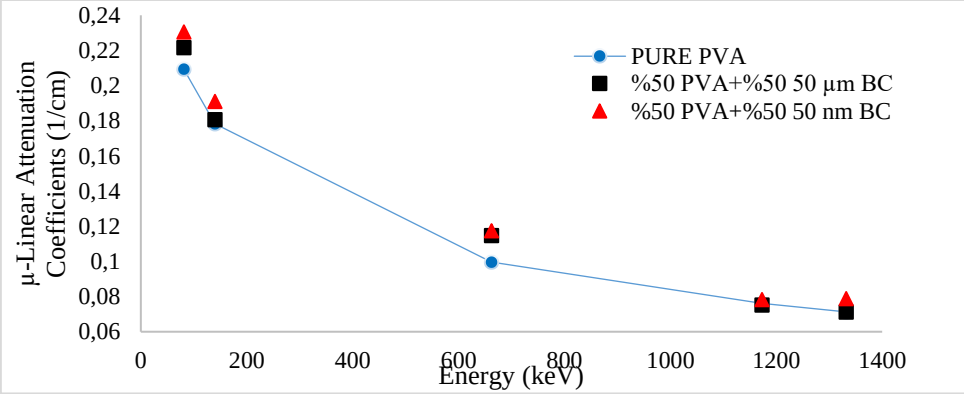


**Figure 6.** Linear Attenuation Coefficients of New Materials Created by Adding Pure PVA and 50% Nano and Micro Sized BC Particles into the PVA Matrix

### *3.4. MFP, HVL, and TVL Values*

The MFP, HVL and TVL values for the 50 nm-BC and 50 μm-BC materials added to PVA in this study are presented in Figure 8.

The MFP value increases with energy because lower-energy photons can lose their energy over short distances, while higher-energy photons require larger distances to lose their energy. As shown in Figure 7 (a), the highest MFP value is achieved with micro-sized BC at 1332 keV energy. HVL is an essential parameter for radiation shielding materials, and the effectiveness of a shielding material against radiation is inversely proportional to its HVL. Figure 7 (b) displays HVL values for PVA with nano and micro-sized BC. Here, micro-sized BC exhibits the highest HVL value at 1332 keV. Figure 7 (c) illustrates the TVL values. Similar to HVL, micro-sized BC added to PVA provides the highest TVL value at 1332 keV.

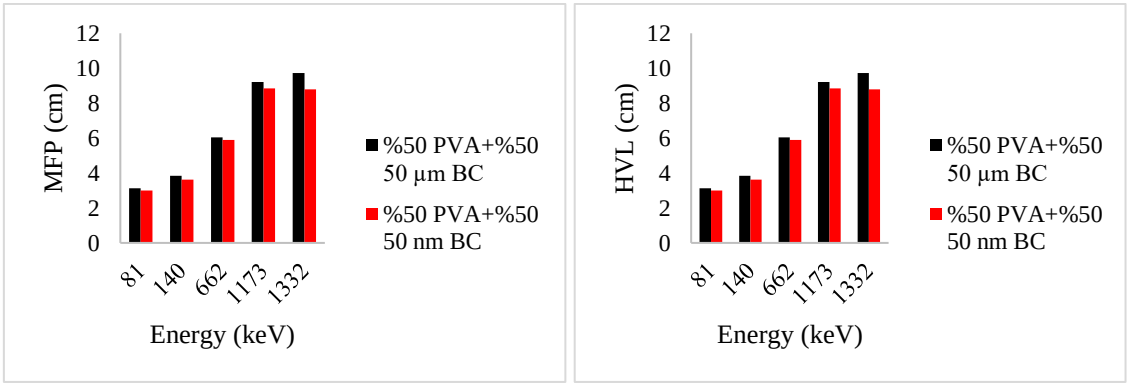


**(a)** **(b)**

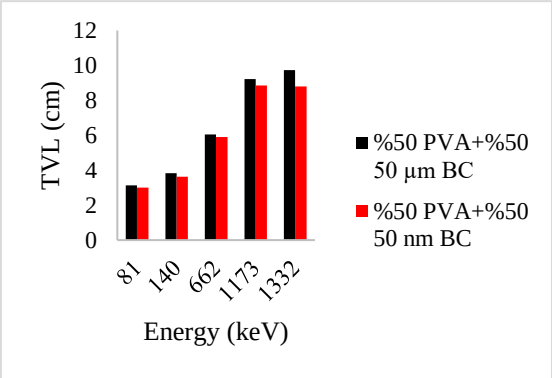


**(c)**

**Figure 7:** Energy-Dependent Changes of MFP (a), HVL (b) And TVL (c) for PVA/Bentonite Clay Forms Created with Nano/Micro Additives

## 4. Discussion and Conclusion

The Bentonite Clay simulated during this study was obtained from Cape Town [27] and effects of this BC on radiation protection has not been investigated before, and no previous study has examined the change in linear attenuation coefficient with particle size. To validate this simulation, linear attenuation coefficient values for pure PVA were calculated and compared with the theoretical results from XCOM NIST, demonstrating the accuracy of the simulation with a 0.43% error margin. During this study, BC was added to PVA to create a homogeneous distribution with a weight fraction of %50 and particle sizes of 50 nm and 50 µm to investigate the effect of particle size and LAC, HVL, MFP, and TVL values were investigated using MCNPX for mono-energetic gamma sources at 81 keV, 140 keV, 662 keV, 1173 keV, and 1332 keV. In [11], gamma energies of 662, 1173, and 1332 keV were investigated, while in this study, the energy range was extended to include 81 keV and 140 keV where photoelectric effect is dominant as a interaction type of matter with photons. Table 3 presents linear attenuation coefficients of four different clays obtained in [11] with LACs for ordinary concrete from [27], and LACs for the BC used in this study are also included. At 662 keV gamma energy, [11] reported that the LACs of Bentonite Clay and Red Clay are equal, and both clays have higher LAC values compared to the other two clays. When compared to ordinary concrete, all clays provide approximately %5.9 better protection at this energy. However, BC used in this study, shows a %27 higher LAC value compared to ordinary concrete. At 1173 keV gamma energy, [11] reported that red clay has the highest LAC value among the clays, but ordinary concrete has a %10.3 higher LAC value compared to red clay. When compared to ordinary concrete, the BC used in this study is approximately %19 more effective. At 1332 keV gamma energy, [11] reported that bentonite clay has the highest LAC value among the clays, while ordinary concrete has a %10.3 higher LAC value compared to bentonite clay. According to the results of this study, it is approximately 19% more effective than ordinary concrete. Table 3 and Figure 4 show that the BC from Cape Town has the highest impact among the energies studied. The fact that bentonite clay samples sometimes show protection performance similar to or even higher than common radiation shields demonstrates their potential in shielding applications. The results show that the highest linear attenuation coefficient is obtained in terms of particle size, in the nano size, and this continues for each energy value. It is because of the materials at the nanometer scale have a significantly larger surface area compared to micro-sized particles with the same mass or volume. This increased surface area provides more opportunities for interactions with radiation, enhancing both scattering and absorption chances, making it highly suitable for gamma ray protection. Due to the results of LAC, the highest HVL value is provided by micro-sized BC at 1332 keV. Since high energy already requires the protective shield to be thicker than low

energies, the shield made with nm-BC is thinner than the shield prepared with μm-BC, as shown in Figure 6. Similar results can be seen for TVL and MFP values in Figure 7 (b)-(c).

As a conclusion, due to its superior performance compared to commonly used concrete for shielding, this clay sample is considered suitable for use as a radiation shielding material by incorporating it into different scenarios. Additionally, using it in nanometer size enhances its effectiveness in protection against gamma radiation. Considering its abundance, applicability, and cost-effectiveness, this material can be utilized in various fields where radiation shielding is required.

### *Authorship contribution statement*

**T.Manici**: Conceptualization, Methodology, MCNP Simulation, Data Curation, Original Draft Writing; **B.Demir**: Conceptualization, Methodology, Visualization, Supervision, Observation, Advice; **N.Akçay, G.Algün**: Visualization, Supervision, Observation, Advice.

### *Declaration of competing interest*

The authors declare that they have no known competing financial interests or personal relationships that could have appeared to influence the work reported in this paper.

### *Ethics Committee Approval and/or Informed Consent Information*

As the authors of this study, we declare that we do not have any ethics committee approval and/or informed consent statement.

## References

[1] M. Asgari, H. Afarideh, H. Ghafoorifard, E. A. Amirabadi, ‘‘Comparison of nano/micro lead, bismuth and tungsten on the gamma shielding properties of the flexible composites against photon in wide energy range (40 keV–662 keV)’’, *Nuclear Engineering and Technology*, 53, 4142-4149, 2021.

[2] S. Nambiar, J. T. W. Yeow, ‘‘Polymer-Composite Materials for Radiation Protection’’, *ACS Applied Materials & Interfaces*, 4, 5717−5726, 2012.

[3] C. Song, J. Zheng, QP. Zhang, YT. Li, YJ. Li, Y. Zhou, ‘‘Numerical simulation and experimental study of PbWO4/EPDM and Bi2WO6/EPDM for the shielding of γ-rays’’, *Chinese Physics C*, 40(8), 089001, 2016.

[4] Y. Dong, SQ. Chang, HX. Zhang, C. Ren, B. Kang, MZ. Dai, YD. Dai, ‘‘Effects of WO3 Particle Size in WO3/Epoxy Resin Radiation Shielding Material’’ *Chinese Physics Letters,* 29(10), 108102, 2012.

[5] H.O. Tekin, V.P. Singh, T. Manici, ‘‘Effects of micro-sized and nano-sized WO3 on mass attenauation coefficients of concrete by using MCNPX code’’, *Applied Radiation and Isotopes*, 121, 122-125, 2017.

[6] H. Alavian, H. Tavakoli-Anbaran, ‘‘Study on gamma shielding polymer composites reinforced with different sizes and proportions of tungsten particles using MCNP code’’, *Progress in Nuclear Energy*, 115, 91–98, 2019.

[7] Y. Karabul, O. İçelli, ‘‘The assessment of usage of epoxy based micro and nano-structured composites enriched with Bi2O3 and WO3 particles for radiation shielding’’, *Results in Physics*, 26, 104423, 2021.

[8] I. Z. Hager, Y. S. Rammah, H. A. Othman, E. M. Ibrahim, S. F. Hassan, F. H. Sallam, ‘‘Nano-structured natural bentonite clay coated by polyvinyl alcohol polymer for gamma ray attenuation’’, *Journal of Theoretical and Applied Physics*. 13, 141–153, 2019.

[9] M. M. Bani-Ahmad, N. Z. N. Azman, J. N. Z. Jasmine, H. M. Almarri, M. Alshipli, M. R. Ramzun, ‘‘Radiation attenuation ability of bentonite clay enriched with eggshell as recyclable waste for a physical rradiation barrier’’, *Radiation Physics and Chemistry*, 201, 110484, 2022.

[10] R. S. Özakar, M. Kara, A. Maman, ‘‘Preparation, characterization, and radiation absorption study of bentonite clay included soft chewable lozenge formulations’’, *Journal of Pharmaceutical Technology* 1(3), 54-59, 2020

[11] M. Elsafi, Y. Koraim, M. Almurayshid, F. I. Almasoud, M. I. Sayyed, I. H. Saleh, ‘‘Investigation of Photon Radiation Attenuation Capability of Different Clay Materials’’, *Materials*. 14, 6702, 2021.

[12] F. Sallam, E. Ibrahim, S. Hassan, A. Omar, ‘‘Shielding properties enhancement of bentonite clay nano particles coated by polyvinyl alcohol polymer’’, *Research Square*, 2021.
[13] T. S. Gaaz, A. B. Sulong, M. N. Akhtar, A. A. Kadhum, A. B. Mohamad, A. A. Al-Amiery, ‘‘Properties and Applications of Polyvinyl Alcohol, Halloysite Nanotubes and Their Nanocomposites’’, *Molecules*. 20, 22833–22847, 2015.
[14] M. Aslam, M. A. Kalyar, Z. A. Raza, ‘‘Polyvinyl Alcohol: A Review of Research Status and Use of Polyvinyl Alcohol Based Nanocomposites’’, *Polymer Engineering and Science*, 58, 2119-2132, 2018.
[15] G. B. Pour, L. F. Aval, M. Mirzaee, ‘‘Flexible graphene supercapacitor based on the PVA electrolyte and BaTiO3/PEDOT:PSS composite separator’’, *Journal of Materials Science:Materials in Electronics*, 29, 17432–17437, 2018.
[16] L. F. Aval, M. Ghoranneviss, G. B. Pour, ‘‘High performance supercapacitors based on the carbon nanotubes, graphene and graphite nanoparticles electrodes’’, *Heliyon*, 4, e00862, 2018.
[17] L. Chang, Y. Zhang, Y. Liu, J. Fang, W. Luan, X. Yang, W. Zhang, ‘‘Preparation and characterization of tungsten/epoxy composites for γ-rays radiation shielding’’, *Nuclear Instruments and Methods in Physics Research Section B*, 356–357, 88-93, 2015.
[18] S. Malekie, N. Hajiloo, ‘‘Comparative Study of Micro and Nano Size WO3/E44 Epoxy Composite as Gamma Radiation Shielding Using MCNP and Experiment’’, *Chinese Physics Letters*, 34, 108102, 2017.
[19] F. Kazemi, S. Malekie, M. A. Hosseini, ‘‘A Monte Carlo Study on the Shielding Properties of a Novel Polyvinyl Alcohol (PVA)/WO3 Composite, Against Gamma Rays, Using the MCNPX Code’’, *Journal Of Biomedical Physics & Engineering*, 9(4), 465-472, 2019.
[20] S. El-Fiki, S. U. El Kameesy, D. E. El. Nashar, M. A. Abou- Leila, M. K. El-Mansy, M. Ahmed, ‘‘Influence of Bismuth Contents on Mechanical and Gamma Ray Attenuation Properties of Silicone Rubber Composite’’, *International Journal of Advanced Research*, 3, 1035-1039, 2015.
[21] H. O. Tekin, V. P. Singh, U. Kara, T. Manici, E. E. Altunsoy, ‘‘Investigation of Nanoparticle Effect on Radiation Shielding Property Using Monte Carlo Method’’, *CBU Journal of Science*, 12 (2), 195-199, 2016.
[22] R. Bagheri, A. K. Moghaddam, H. Yousefnia, ‘‘Gamma Ray Shielding Study of Barium–Bismuth–Borosilicate Glasses as Transparent Shielding Materials using MCNP-4C Code, XCOM Program, and Available Experimental Data’’, *Nuclear Engineering and Technology*, 9, 216-223, 2017.
[23] MCNPX 240, Monte Carlo N-Particle Transport Code System for Multiparticle and High Energy Applications (Sep 2004). Bibliographic information available from INIS: http://inis.iaea.org/search/search.aspx?orig_q=RN:39098954 Available on-line: http://www.nea.fr/abs/html/ccc-0715.html
[24] K. Verdipoor, A. Alemi, A. Mesbahi, ‘‘Photon mass attenuation coefficients of a silicon resin loaded with WO3, PbO, and Bi2O3 Micro and Nano-particles for radiation shielding’’, *Radiation Physics and Chemistry*, 147, 85–90, 2018.
[25] J. K. Shultis, R. E. Faw, ‘‘An MCNP Primer’’, *Dept. of Mechanical and Nuclear Engineering Kansas State University Manhattan*, KS 66506.
[26] M. Vhahangwele, G. W. Mugera, N. Tholiso, ‘‘Defluoridation of drinking water using Al3+-modified bentonite clay: optimization of fluoride adsorption conditions’’, Toxicological & Environmental Chemistry, 96(9), 1294-1309, 2014.
[27] M.J. Berger, J.H Hubbell, S.M. Seltzer, J. Chang, J.S. Coursey, R. Sukumar, D.S. Zucker, K. Olsen, XCOM: Photon Cross Section Database. National Institute of Standards and Technology (NIST). Published 2010. Available online: http://physics.nist. gov/xcom.
[28] I. I. Bashter, ‘‘Calculatıon of Radıatıon Attenuatıon Coefficıents For Shıeldıng Concretes’’, *Annals of Nuclear Energy*, 24 (17), 1389-1401, 1997.